Flexible beam in R^3 under large overall motions and Asynchronous Variational Integrators

François DEMOURES
PhD-student
EPFL
Lausanne, Suisse
francois.demoures@epfl.ch

François GAY-BALMAZ
CNRS Researcher
Ecole Normale Supérieure
Paris, France
gaybalma@lmd.ens.fr

Julien NEMBRINI
Scientific Researcher
Universität der Künste
Berlin, Germany
julien.nembrini@epfl.ch

Tudor RATIU
Chaired Professor
EPFL
Lausanne, Suisse
tudor.ratiu@epfl.ch

Yves WEINAND
Associate Professor
EPFL
Lausanne, Suisse
yves.weinand@epfl.ch

Summary

The goal of this note is to present some new results on the application of AVI algorithms to the Simo-Marsden-Krishnaprasad beam model based on a description using rotation matrices. This follows our earlier work on the Euler-Bernoulli beam and thin-shell models with Kirchhoff-Love constraints and various boundary conditions. We consider the effect of large deflections, when the beam is subject to constraints, with different boundary conditions, and show that we can use the properties of the AVI to adapt the time-step to the constraints.

Keywords: discrete variational mechanics, AVI, beam, special Cosserat rod, frame-indifference, Lie group variational integrator.

1. Introduction

The AVI method is used to carry out dynamic and static two-dimensional simulations. To simulate the dynamics towards and equilibrium state, we employ the discrete version of the Lagrange-d'Alembert principle to a non-conservative system with dissipation. This gives ultimately the equilibrium position of the system.

Firstly, we consider a Bernoulli plane-beam model. Our goal is to study the influence of time steps on the dynamic behavior of stress areas, such as near boundaries or edges. It may be possible to improve the computing speed and performance by reducing the time interval in areas under stress and increasing it elsewhere. This adjustment of the time step according to the singularities may have an influence on the trajectories of nodes and on the instabilities. This is an important problem in the study of the dynamics of complex structures in civil engineering.

Secondly, we review from Simo, Marsden, and Krishnaprasad [2], the kinematic description of a beam in ambient Euclidean space $\mathbf{R}^3$. We present the Lagrangian representation of the motion of a beam of length L by taking the configuration space to be $C^\infty([0,L], SE(3))$. After space and time discretization, we get a variational integrator; the strain of the corresponding discrete model remains objective (frame-indifferent). This is a fundamental property of three-dimensional elasticity which can be violated by certain interpolations of rotations. We obtain an asynchronous variational integrator well adapted to the study of constrained beam dynamics subject to large deformations. The inherent property to preserve the symmetries allows us to properly define the equilibrium position.

2. Time intervals in areas under stress and AVI

2.1 Variational integrator for the Bernoulli beam

The bending energy function of the displacement field u for a Bernoulli beam element of length L is

$$W(u) = \frac{1}{2} \int_0^L EI \left(\frac{\partial^2 u}{\partial S^2} \right)^2 dS \qquad (1)$$

where E is Young's modulus and I is the second moment of the cross section.

We discretize the interval [0, L] by N one-dimensional subintervals K of [0, L]. To each element K corresponds a set of nodes a in K. Of course, one node can belong to two elements. We use three models of polynomial approximation and, therefore, three models of shape functions, for each beam element K. The first is associated to quadratic uniform B-splines, the second to cubic uniform B-splines, and the third to Hermitian cubic shape functions.

For a general Lagrangian which is the difference of the kinetic energy and potential energy $V_K(u)$ of the element K, we construct the following discrete Lagrangian:

$$L_K^j\left(u_K^j, u_K^{j+1}\right) = \sum_{a \in K} \sum_{t_K^j \le t_a^j \le t_K^{j+1}} \frac{1}{2} m_{K,a} \left(t_a^{i+1} - t_a^i\right) \left\| \frac{u_a^{i+1} - u_a^i}{t_a^{i+1} - t_a^i} \right\|^2 - \left(t_K^{j+1} - t_K^j\right) V_K\left(u_K^{j+1}\right) \qquad (2)$$

where u_a^j and u_a^{j+1} are two displacements at times t_a^j and t_a^{j+1}(see Lew et al. [3]). In the particular case of the Bernoulli beam, the potential energy is the sum of the elastic potential energy $W(u)$ and the potential energy of distributed loading. For example, using quadratic B-splines, we obtain the following one-step integrator

$$\left[\left(\frac{u_K^{i+1} - u_K^i}{t_{u_K}^{i+1} - t_{u_K}^i} \right) - \left(\frac{u_K^i - u_K^{i-1}}{t_{u_K}^i - t_{u_K}^{i-1}} \right) \right] = - \left(t_K^j - t_K^{j-1}\right) M_K^{-1} \left(\left(\frac{l}{4} EI \int_0^1 B^T B d\xi \right) u_K^j - \frac{1}{2} ql \int_0^1 N d\xi \right)_{t_{u_K}^i = t_K^j}, \qquad (3)$$

where $u_K^i = \left(u_a^i,\ u_{a+1}^i,\ u_{a+2}^i\right)^T$ is the nodal vector displacement for each node a in K at time t_a^j.

2.2 Experimentation

The beam starts in a horizontal straight position and oscillates, possibly reaching equilibrium due to damping. In all the experiments below, a 10 elements mesh with equal length is used with beam dimensions 1 x 0.01 x 0.02 in meters (L x h x w) consisting of a homogeneous isotropic material (E=109, ρ=400 kg/m3, υ= 0.3). To set the time stepping, we make use of the Courant limit

$$\Delta t = f \frac{h}{\sqrt{\frac{\lambda_0 + 2\mu_0}{\rho}}}, \qquad (4)$$

where h is the radius of the largest ball contained in the element, ρ is the density, and λ_0, μ_0 are the Lamé coefficients of the simulated material (see [3]). In setting f, it is possible to tune the accuracy of the trajectories in order to explore the limits of stability. Our goal is to adapt the time step to the size of the mesh, or near boundaries and contact points for a given regular mesh. We consider this experimental study as a complement to the work of Fong, Darve, and Lew [4].

The focus is on heterogeneous time rather than space subdivisions, hence the use of elements K with equal lengths. Additional manipulation would be needed to account for differing element sizes.

However, in order to avoid integration artifacts, possibly arising with unwanted synchronization, we introduce a 1% randomness on the time steps computed according to the Courant fraction to ensure different time steps between elements.

As a main topic of interest, we explore the potential of AVI to allow higher integration speed in regions displaying less constraints, by gradually increasing f for elements located in the middle of the beam. Our results are compared against standard Courant fraction time stepping ($f = 1$) and double integration speed ($f = 2$). These different sets of time steps are depicted in Figure (1).

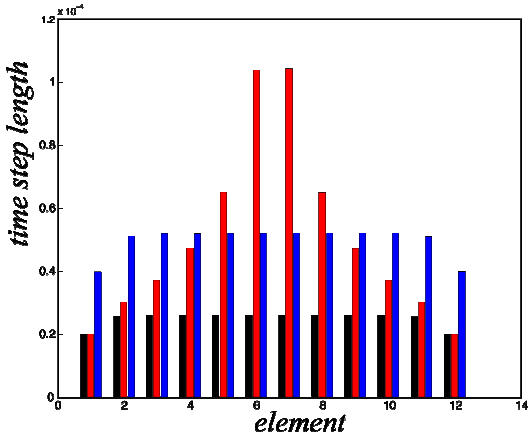

Fig. 1: Variation on time-stepping along the beam

Lew et al. [3] studied the computational cost and established AVI as substantially cheaper than the Newmark algorithm. We show that the heterogeneous time-stepping strategy can further lower this computational cost while achieving acceptable results.

2.2.1 Statics results

We firstly observe that with Hermitian cubic shape functions the AVI is able to reach very acceptable precision for all boundary conditions considered, when using standard time-stepping with Courant fraction ($f = 1$). Secondly, we note that the heterogeneous time-stepping performs rather poorly in comparison to standard time-stepping.

With quadratic B-splines, in the case of standard time-stepping, the correspondence with analytical results is again quite remarkable. Looking at the influence of the time-stepping scheme, we note that non-standard time steps perform slightly better than in the Hermitian case.

Finally with cubic B-splines, in the case of standard time-stepping, the correspondence with analytical results is again quite remarkable. Looking at the influence of the time-stepping scheme, we note that non-standard time steps perform much better than with previous shape functions.

2.2.2 Dynamics results

Considering cubic Hermitian shape functions, they tend to desynchronize over time, revealing differing periods. The difference is more important in the case of the heterogeneous time steps.

For quadratic B-splines, the desynchronization seems to show a lower magnitude.

The case of cubic B-splines is more interesting in the sense that the desynchronization is much lower than for the previously considered shape functions. The heterogeneous time-stepping is stable for all boundary conditions, whereas the accelerated time-stepping ($f = 2$) displays instabilities for the fixed-end case. This shows that it is possible to profit from the AVI potential for local integration acceleration without loss of stability. However the influence on the dynamics of such an approach still needs to be better understood.

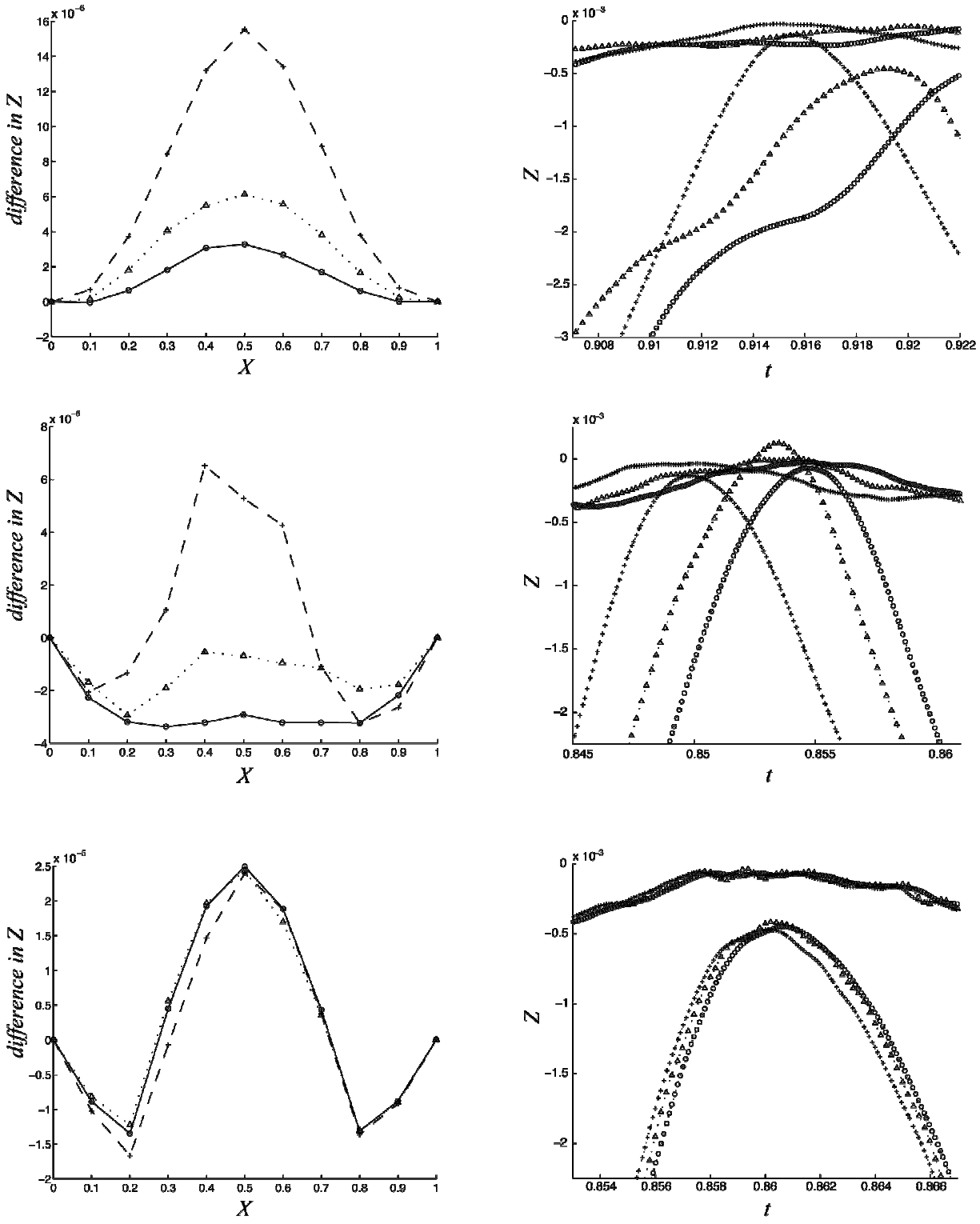

Fig. 2: From top to bottom: Hermitian cubic, quadratic B-spline and cubic B-spline shape functions. Static difference to analytical result (left) for fixed-end and close-up of dynamic trajectories (right) for a node on the edge of the beam (x=0.1) for cantilever. (○) time stepping computed with f=1, in (Δ) time stepping computed with f=2, (+) heterogeneous time-stepping.

3. Flexible beam in $\mathbf{R}^3$ under large overall motions and AVI.

3.1 Lagrangian dynamics of the beam in $\mathbf{R}^3$

3.1.1 Deformation expressed relative to the inertial frame

We first review from [2] the kinematic description of a beam in the ambient space $\mathbf{R}^3$. The configuration of a beam is defined by specifying the position of its line of centroids by means of a map ϕ: $[0,L] \to \mathbf{R}^3$, and the orientation of cross-sections at points $\phi(S)$ by means of a moving basis $\{\mathbf{d}_1(S), \mathbf{d}_2(S), \mathbf{d}_3(S)\}$ attached to the cross section. The orientation of the moving basis is described with the help of an orthogonal transformation Λ: $[0,L] \to SO(3)$ such that

$$d_I(S) = \Lambda(S) E_I, \quad I = 1, 2, 3 \qquad (5)$$

where $\{\mathbf{E}_1, \mathbf{E}_2, \mathbf{E}_3\}$ is a fixed basis referred to as the *material frame*. The configuration of the beam is thus completely determined by the maps ϕ and Λ in the configuration space

$$G = C^\infty([0,L],\ SE(3)), \quad \text{with} \quad \Phi = (\Lambda,\ \phi),$$

which is a Lie group; $SE(3)$ denotes the Euclidean group. If boundary conditions are imposed, then they need to be included in this configuration space. Suppose that the cross section is given by a compact subset $\mathcal{A}$ of $\mathbf{R}^2$ with smooth boundary. Then the set occupied by the beam is

$$B = \{X \in \mathbf{R}^3 \mid X = \phi(S) + \sum_{\alpha=1}^{2} \xi^\alpha \Lambda(S) E_\alpha, \text{ with } (\xi^1,\ \xi^2,\ S) \in \mathcal{A} \times [0,L]\ \}.$$

For simplicity, we assume that $\phi(S)$ is passing through the center of mass of the cross section $\mathcal{A}$. The *material velocity* $V_\phi \in T_\phi G$ is defined by

$$V_\phi(S,\ t) = \frac{d}{dt}\Phi(S,\ t) = (\dot{\Lambda}(S,\ t),\ \dot{\phi}(S,\ t)). \qquad (6)$$

The convected velocity field is

$$\upsilon_\phi(S,t) := (\Lambda^{-1}(S,t)\dot{\Lambda}(S,t),\ \Lambda^{-1}(S,t)\dot{\phi}(S,t)) = (\hat{K},\ \gamma) \qquad (7)$$

which is an element of the Lie algebra $se(3)$. It is important to note that $\dot{\Lambda} = \Lambda\hat{K}$ is the attitude kinematics equation of a rigid body, where Λ is the rotation matrix from the body-fixed frame to the reference frame and K is the angular velocity of the rigid body represented in the body fixed frame.

Throughout this work, we will use the standard Lie algebra isomorphism ^ between ($\mathbf{R}^3$, x) and ($so(3)$, [,]), called the *hat map* (see Marsden and Ratiu [5]).

The kinetic energy of the beam is found by integrating the kinetic energy of the material points over the whole body. Given $\mathcal{D} = [0,\ L] \times \mathcal{A}$, we have

$$T(\phi,\ \dot{\phi},\ \Lambda,\ \dot{\Lambda}) = \frac{1}{2}\int_D \left\| \dot{\phi} + \Lambda\hat{K}(\xi^1 E_1 + \xi^2 E_2) \right\|^2 \rho(S,\ \xi^1,\ \xi^2)\, dS d\xi^1 d\xi^2$$

$$= \frac{1}{2}\int_0^L M\|\gamma\|^2 dS + \frac{1}{2}\int_0^L Tr\left[\hat{K} J_d \hat{K}^T\right] dS, \qquad (8)$$

where

$$J_d = \int_{\mathcal{A}} \rho\, (\xi^1 E_1 + \xi^2 E_2)(\xi^1 E_1 + \xi^2 E_2)^T d\xi^1 d\xi^2. \qquad (9)$$

Given a configuration $(\Lambda,\ \phi) \in\ G$, the convected strains are

$$(\hat{W},\ \Gamma) := (\Lambda^{-1}\Lambda',\ \Lambda^{-1}\phi'). \qquad (10)$$

The bending energy is assumed to depend on the deformation gradient only through the quantity W and Γ, that is, we have

$$\Pi_{\text{int}}(\Lambda,\ \phi) = \int_0^L \Psi(W,\ \Gamma)\ dS, \qquad (11)$$

where $\Psi(W,\ \Gamma)$ is the stored energy function. We assume that the unstressed state is not stretched and not sheared. Also, by taking into account that the thickness of the rod is small compared to its length and that the material is homogenous and isotropic, we can consider, as in Dichmann, Li, and Maddocks [6], the stored energy to be given by the following quadratic model

$$\Psi(W,\ \Gamma) = \frac{1}{2}\left[(\Gamma - E_3)^T C_1(\Gamma - E_3) + W^T C_2 W\right] \qquad (12)$$

where

$$C_1 := \begin{pmatrix} GA_1 & 0 & 0 \\ 0 & GA_2 & 0 \\ 0 & 0 & EA \end{pmatrix} \quad \text{and} \quad C_2 := \begin{pmatrix} EI_1 & 0 & 0 \\ 0 & EI_2 & 0 \\ 0 & 0 & GJ \end{pmatrix}, \qquad (13)$$

$GA_1,\ GA_2,\ EA,\ EI_1,\ EI_2,\ GJ$, are the elasticity coefficients, $A_1 = A_2 = A$, $J = I_1 + I_2$, A is the cross-sectional area of the rod, E is Young's modulus, $G=E/\{2(1+\upsilon)\}$ is the shear modulus, and υ is Poisson's ratio.

Let $L : TG \to \mathbf{R}$ be a Lagrangian (kinetic minus potential energy) defined on the tangent bundle TG of a Lie group G. Using the left trivialization $TG \cong G \times \mathfrak{g}$ of the tangent bundle, where $\mathfrak{g}$ is the Lie algebra of the Lie group G, we get a function $\mathcal{L} : G \times \mathfrak{g} \to \mathbf{R}$ defined by

$$\mathcal{L}(g,\xi) := L(g, \dot{g}), \qquad \dot{g} := g\xi. \qquad (14)$$

Therefore, in the case of the beam, the *trivialized Lagrangian* $\mathcal{L}(g,\xi)$ on

$$G \times \mathfrak{g} = C^\infty([0,\ L],\ SE(3)) \times\ C^\infty([0,\ L],\ \mathfrak{se}(3))$$

has the expression

$$\mathcal{L}(\Lambda,\ \phi,\ \hat{K},\ \gamma) = \frac{1}{2}\int_0^L M\|\gamma\|^2 dS + \frac{1}{2}\int_0^L Tr\left[\hat{K} J_d \hat{K}^T\right] dS - \Pi_{\text{int}}(\Lambda,\phi) - \Pi_{ext}(\phi). \qquad (15)$$

3.1.2 Spatial discretization and objectivity

We discretize the interval [0, L] by N elements, such that for one element K of unit length with two nodes we have

$$\Lambda_h(S) = \Lambda_a \exp(S\hat{\psi}_a), \qquad \phi_h(S) = x_a + S\Delta x_a, \qquad (16)$$

where $\Lambda_{a+1} := \Lambda_h(1) = \Lambda_a \exp(\hat{\psi}_a)$, and $x_{a+1} := \phi_h(1) = x_a + \Delta x_a$. So the variables in the spatially discretized Lagrangian are the rotation matrices $\Lambda_K = (\Lambda_a, \Lambda_{a+1})^T$ and the position of the nodes $x_K = (x_a, x_{a+1})$, at a and $a+1$.

We know from Crisfield and Jelenic [7] that this spatial discretization provides an objective strain measure, whereas with a linear interpolation of the rotational vector we lose the objectivity.

The trivialized form of the spatially discretized Lagrangian is obtained by inserting these variables in the continuous trivialized Lagrangian and by considering the approximation. We find

$$\mathcal{L}_K(\Lambda_K,\ x_K,\ \dot{\Lambda}_K,\ \dot{x}_K) = \frac{1}{4}M\left(\|\gamma_a\|^2 + \|\gamma_{a+1}\|^2\right) + \frac{1}{4}\left(Tr\left(\hat{K}_a J_d (\hat{K}_a)^T\right) + Tr\left(\hat{K}_{a+1} J_d (\hat{K}_{a+1})^T\right)\right) + V(x_K, \Lambda_K) \qquad (17)$$

where $K_K = (K_a,\ K_{a+1})^T$ and $\gamma_K = (\gamma_a,\ \gamma_{a+1})^T$.

3.1.3 Temporal discretization

The configuration of the discretized element K at time t_K^j is described by $g_K^j = (\Lambda_K^j,\ x_K^j) \in SE(3)^{N_K}$, where N_K is the number of nodes a in the element K. We define f_K^j such that $g_K^{j+1} = g_K^j f_K^j$ and hence we have

$$f_K^j = (g_K^j)^{-1} g_K^{j+1} = \left((\Lambda_K^j)^{-1}\Lambda_K^{j+1},\ (\Lambda_K^j)^{-1}(x_K^{j+1} - x_K^j)\right) = (F_K^j,\ H_K^j) \qquad (18)$$

The discrete Lagrangian L_K^j defined at time t_K^j associated to the trivialized Lagrangian (17) can be defined by considering the contribution of the K-th element to the discrete reduced Lagrangian over the time interval $[t_K^j,\ t_K^{j+1}]$. The discrete Lagrangian L_K^j is therefore

$$L_K^j(\Lambda_K^j,\ x_K^j,\ F_K^j,\ H_K^j) = \sum_{a \in K} \sum_{t_K^j \le t_a^i \le t_K^{j+1}} \left\{ \frac{1}{4} M (t_a^{i+1} - t_a^i) \left\| \frac{H_a^i}{t_a^{i+1} - t_a^i} \right\|^2 + \frac{1}{2(t_a^{i+1} - t_a^i)} Tr\left[(I_3 - F_a^i)\ J_d\right] \right\} - (t_K^{j+1} - t_K^j)\ V_K(\Lambda_K^j,\ x_K^j) \qquad (19)$$

3.2 Integrator

Our mechanical system evolves on a Lie group. As a consequence, we use the discrete Lagrangian $L_K^j : G \times G \times \mathbf{R} \to \mathbf{R}$ given in (19) and discrete Euler-Lagrange equations or the Lie group variational integrator developed by Lee [8].

For the calculation of these equations, we will consider that $t_a^i = t_K^j$ for $a \in K$ (this assumption will imply special handling when implementing to get an asynchronous variational integrator as described in [3]).

3.3 Implementation

The implementation of this integrator is in progress and the results we will obtain will be compared with those of other integrators for flexible beams in $\mathbf{R}^3$ under large overall motions we have already started to develop.

4. Conclusion

The focus of this note was to present recent achievements in our endeavor to develop a dimensioning tool for dynamic as well static analysis of complex civil engineering structures under constraints. An example in the form of assemblies of pre-stressed bent elements, forming complex textile-like structures, is currently under study at the IBois Laboratory of the EPFL.

We want to take advantage of the excellent accuracy, conservation of geometric properties, and convergence characteristics of AVIs, together with their specific property of heterogeneous time-steps, allowing to shorten them on the boundaries submitted to constraints, as seen in the first part of this paper.

The goal is to use the newly developed geometric integrators presented in the second part of the paper, which preserve the Lie group structure, to study geometrically exact rod mechanics where objectivity is automatically conserved after discretization.

5. References.

[1] MARSDEN J.E., WEST M., "Discrete mechanics and variational integrators", *Acta Numer.*, 10, 2001, pp. 357-514.

[2] SIMO J.C., MARSDEN J.E., KRISHNAPRASAD P. S., "The Hamiltonian structure of nonlinear elasticity: The material, spatial and convective representations of solids rods and plates." *Arch. Rational Mech. Anal.*, 104, 1988, pp. 125-183.

[3] LEW A., MARSDEN J.E., ORTIZ M., WEST M., "Variational time integrators." *Internat. J. Numer. Methods Engrg.*, 60(1), 2004, pp. 153-212.

[4] FONG D., DARVE E., LEW A., "Stability of Asynchronous Variational Integrators." *J. Comput. Physics.*, 227, 2008, pp. 8367-8394.

[5] MARSDEN J. E., RATIU T. S., *Introduction to Mechanics and Symmetry*. 2nd edition, Springer, 1999, p 289.

[6] DICHMANN D., LI Y., MADDOCKS J. H., "Hamilton formulation and symmetries in rod mechanics. In "Mathematical Approaches to Biomolecular Structure and Dynamics." (Minneapolis, MN, 1994), Volume 82 of IMA Math. Appl., Springer, New-York, 1996, pp. 71-113.

[7] CRISFIELD M.A., JELENIC G., "Objectivity of strain measures in the geometrically exact three-dimensional beam theory and its finite-element implementation." The Royal Society, Imperial College, 1998, pp. 1125-1147.

[8] LEE T., *Computational Geometric Mechanics and Control of Rigid Bodies*. Ph.D. Thesis, University of Michigan, 2008, pp. 55-56.